

Fabrication and characterization of Er,Nd codoped Y₂O₃ Transparent Ceramic: A dual mode Photo-luminescence emitter

Pratik Deshmukh^{a,*}, S. Satapathy^{a,c*}, Anju Ahlawat^a, M K Tiwari^b and A. K. Karnal^{a,c}

^a Laser Materials Section, Raja Ramanna Centre for Advanced Technology, Indore 452013, India

^b Synchrotron Utilization Section, Raja Ramanna Centre for Advanced Technology, Indore 452013, India

^cHomi Bhabha National Institute, BARC, Mumbai, India.

Corresponding author

* E- mail: ppdeshmukh@rrcat.gov.in; srinu73@cat.ernet.in

Phone: 91 731 2442905/2920/2010

Fax: 91 731 2442900

Abstract:

The transparent Er, Nd co-doped Y₂O₃ ceramics with transparency ~78% (in 500-2000 nm range without Fresnel's correction) were fabricated successfully. It involved nanoparticle synthesis by coprecipitation method and sintering of pellets under high vacuum condition. The crystalline phase, particle size and element composition were confirmed by X-ray diffraction, scanning electron microscope, energy dispersive X-ray fluorescence techniques, respectively. The upconversion luminescence mechanisms involving energy transfer and non-radiative relaxation were analyzed. It is expected that, the result evolved from this study will provide better understanding of upconversion mechanism involved in Er, Nd codoped host material. The emission at both 563 nm (Er³⁺:⁴S_{3/2} →⁴I_{15/2}) and 1064 nm (Nd³⁺:⁴F_{3/2} →⁴I_{9/2}) on 822 nm (Nd³⁺:⁴I_{9/2}→⁴F_{5/2}) excitation proves potential of the ceramic material for dual mode efficient emitter.

1. Introduction

The transparent ceramics application as a laser gain medium has increased after the evolution of thin disk laser concept. This concept is based on a laser design for the diode pumped solid state lasers, which leads to achieve high efficient laser oscillations in compact device [1-2]. The transparent ceramic of various materials such as Y_2O_3 , YAG, Sc_2O_3 and La_2O_3 were already well fabricated [3-6]. The high transmittance in wide spectral range (i.e. from visible to Infra-red) proves transparent ceramic's potential for upconversion (UC) laser application [7].

Upconversion is anti-stoke emission type process referred as nonlinear optical process where sequential absorption of two or more photons leads to emission of a single photon having shorter wavelength than that of incident one [8]. It has advantages over other nonlinear optical process such as second harmonic generations because of no strict requirement of coherent excitation source, phase matching condition and operation at comparatively low incident power [9-10].

Amongst the various dopant in solid state materials, most efficient UC emission occurs with rare earth ions [8]. However, Laporte-forbidden transition (i.e. 4f-4f) limits the absorption of incident light. The increase in dopant concentration increases the absorption up-to a limit over which cross-relaxation dominates. The use of sensitizer in lanthanide doped phosphor is often preferred, which is a strong absorbing ion and transfer the energy to activator efficiently.

The Er^{3+} based upconversion phosphor is widely used with Yb^{3+} , which acts as sensitizer for 980 nm excitation wavelength. The energy difference between $^2F_{7/2}$ to $^2F_{5/2}$ transition of Yb^{3+} matched well with several f-f transitions in Er^{3+} . Thus, allowing resonant energy transition between them [8,11]. Similarly, Nd^{3+} doped material mostly utilized for efficient laser oscillator. In addition, the absorption cross-section of Nd^{3+} around 808 nm is much larger (about 10 times) compared to Yb^{3+} ions at 980 nm [12]. Nd^{3+} and Er^{3+} codoped nanophosphor for bioimaging in dual mode (i.e. emission in visible and IR region simultaneously) on 800 nm excitation have been reported by Li et al [13]. Thus, its use as sensitizer not only improve efficiency of upconversion process but also leads to dual mode emitter as described in fig. 1.

In this paper, Nd and Nd, Er codoped Y_2O_3 transparent ceramics were fabricated by utilizing vacuum sintering for densification of nanoparticles synthesized by co-precipitation method. Subsequently, the photoluminescence characterization has been studied. The upconversion

mechanism leading to intense emission at 563 nm ($\text{Er}^4\text{S}_{3/2} \rightarrow ^4\text{I}_{15/2}$) on 822 nm ($\text{Nd}^4\text{I}_{9/2} \rightarrow ^4\text{F}_{5/2}$) excitation have been investigated. To the best of our knowledge, Er, Nd co-doped Y_2O_3 transparent ceramics fabrication and photoluminescence characterization have not been reported yet.

2. Materials and methods

The nanoparticles synthesis with uniform morphology and narrow particle size distribution is considered as an important parameter involved in the fabrication of transparent ceramics. Here, the co-precipitation method was used to synthesize nano powder of $\text{Er}(x \text{ at\%}), \text{Nd}(1 \text{ at\%}): \text{Y}_2\text{O}_3$ (where, $x=0$ and 1) with additional Zr^{4+} and La^{3+} dopants [14-15]. These additional dopants ($\text{Zr}^{4+}(2 \text{ at\%})$ and $\text{La}^{3+}(1 \text{ at\%})$) acts as sintering additives. Mother solution was prepared by dissolving La_2O_3 , Nd_2O_3 , Er_2O_3 , Y_2O_3 (purity 99.99%) and $\text{ZrOCl}_2 \cdot 8\text{H}_2\text{O}$ (purity 98%) (0.2M) in dilute nitric acid (1.5M). The precipitant ammonium solution was added gradually in nitrate solution under vigorous stirring. Ammonium sulfate solution was used as surfactant, which is added in dispersant solution after an hour of aging. Washing of precipitate was carried out for 5 h using methanol as washing solvent. Further, the washed precipitate was filtered, dried (at 80°C) and calcined at 900°C to get desired oxide powder. This oxide powder was pelletized using uniaxial press and finally vacuum sintered at 1750°C for 5 h.

Rigaku X-ray diffractometer, Zeiss field emission scanning microscope (FESEM) and Malvern Zetastar 90 (model no-ZEN 3690) particle size analyzer were utilized for the characterization of nanoparticles. Chemical composition of the sintered pellets was analyzed using energy dispersive X-ray fluorescence (EDXRF) measurement at BL-16 beamline of Indus-2 synchrotron radiation facility [16]. The quantitative analysis was carried out by Fundamental parameter method using CATXRF program [17]. The sintered specimen was double-side polished (1.0 mm thick) and its optical spectra were measured on a V-670 transmission spectrophotometer (JASCO Corporation). The upconversion and downshifting luminescence spectra were obtained with a FLS920-s fluorescence spectrometer (Edinburgh Instruments Ltd.) upon excitation at 822 nm. All characterizations were performed at room temperature.

3. Result and discussion

The XRD patterns of prepared $\text{Y}_2\text{O}_3:\text{Er}^{3+}(1\text{at}\%)$, $\text{Nd}^{3+}(1\text{at}\%)$ and $\text{Y}_2\text{O}_3:\text{Nd}^{3+}(1\text{at}\%)$ nanopowders along with JCPDS Card No. 41-1105 are shown in fig. 2. The characteristic diffraction peaks of as-prepared samples matched well with the standard cubic Y_2O_3 (JCPDS Card No. 41-1105) phase with space group Ia-3. Also, no additional peak is found in the pattern, indicating that dopants concentrations are under solubility limit.

Figure 3(a) and 3(b), respectively, shows morphology of $\text{Y}_2\text{O}_3:\text{Nd}^{3+}(1\text{at}\%)$ and $\text{Y}_2\text{O}_3:\text{Er}^{3+}(1\text{at}\%)$, $\text{Nd}^{3+}(1\text{at}\%)$ powders after calcination. The particles are physically overlapped and are having nearly spherical morphology. The particle size distribution of the samples, measured using dynamic light scattering method is shown in figure 3(c). The narrow range ($\sim 10\text{-}80\text{ nm}$) of particle size distribution shows the suitability of nanoparticles for transparent ceramic fabrication.

Figure 4(a) and 4(b) shows the characteristic XRF signals of Nd, La, Zr and Y in $\text{Y}_2\text{O}_3:\text{Nd}^{3+}(1\text{at}\%)$ and additional Er signal in $\text{Y}_2\text{O}_3:\text{Er}^{3+}(1\text{at}\%),\text{Nd}^{3+}(1\text{at}\%)$. It consists of characteristic peaks with superimposed spectral artifacts and well-defined background. The Y fluorescent lines (K_α and K_β) are well distinguishable for 19.7 keV excitation energy. Several small peaks in the spectra confirm the presence of various dopant ions Zr, La, Nd and Er in host Y_2O_3 . The elemental composition of both samples $\text{Y}_2\text{O}_3:\text{Nd}^{3+}(1\text{at}\%)$ and $\text{Y}_2\text{O}_3:\text{Er}^{3+}(1\text{at}\%),\text{Nd}^{3+}(1\text{at}\%)$ were determined using XRF measurement and are shown in table1. It matches quit well with the nominal compositions within the predicted error range of XRF technique. The statistical error in peak intensity determination is the dominant error, which varies with element concentration.

The optical transmittance of $\text{Y}_2\text{O}_3:\text{Er}^{3+}(1\text{at}\%),\text{Nd}^{3+}(1\text{at}\%)$ sintered pellet of 1 mm thickness is shown in fig. 5. the Light transmittance is the important parameter for estimating the optical properties of transparent ceramics. The transmittance reached $\sim 78\%$ at 564 nm and almost remains constant at higher wavelengths except at characteristic absorption peaks of dopants. The spectrum consists of various absorption bands originating from ground state of both dopants Nd^{3+} and Er^{3+} . Most of the prominent absorption bands are designated in spectrum. The band centered at 592, 743, 822 and 896 nm are attributed to transition from ground state $^4\text{I}_{9/2}$ to excited states $^2\text{G}_{7/2}+^4\text{G}_{5/2}$, $^4\text{S}_{3/2}+^4\text{F}_{7/2}$, $^2\text{H}_{9/2}+^4\text{F}_{5/2}$ and $^4\text{F}_{3/2}$ of Nd^{3+} , respectively [18]. Also, some well separated absorption peaks of Er^{3+} are observed at 380, 523 and 1536 nm due to ground state ($^4\text{I}_{15/2}$) to $^4\text{G}_{11/2}$, $^2\text{H}_{11/2}$, and $^4\text{I}_{13/2}$ transitions respectively [19-20].

Figure 6(a) shows the infrared excitation spectra of both (Y₂O₃:Er³⁺(1at%)Nd³⁺(1at%)) and Y₂O₃:Nd³⁺(1at%) transparent ceramics. The recorded spectra, on monitoring emission at 1064 nm, shows several prominent excitation peaks around 822 and 895 nm corresponding to transition from ground state ⁴I_{9/2} to excited states ⁴F_{5/2}+²H_{9/2} and ⁴F_{3/2} respectively [18]. The peak positions in excitation spectra are same irrespective of dopants in Y₂O₃ transparent ceramic but relatively lower intensity peaks observed for co-doped sample. This indicates the energy transfer is possible between the corresponding dopants.

Figure 6(b) shows the PL emission spectra, under 822 nm excitation, of Y₂O₃:Er³⁺(1at%)Nd³⁺(1at%) and Y₂O₃:Nd³⁺(1at%) samples in 420 to 1700 nm range. In this measured range for Y₂O₃:Nd³⁺(1at%), three emission bands 870-985 nm, 1040-1196 nm and 1306-1469 nm corresponding to transition from ⁴F_{3/2} to ⁴I_{9/2}, ⁴I_{11/2} and ⁴I_{13/2} energy level of Nd³⁺, respectively, were observed. In the case of co-doped sample (Y₂O₃:Er³⁺(1at%)Nd³⁺(1at%)), additional emission peaks observed at 500, 548, 563, 660 and 1535 nm, which corresponds to transitions from excited levels ⁴F_{7/2}, ²H_{11/2}, ⁴S_{3/2}, ⁴F_{9/2} and ⁴I_{13/2} to ground level ⁴I_{15/2} of Er³⁺ respectively. It is worth noting that there is a significant change in emission intensity of Nd³⁺ band in Er, Nd co-doped Y₂O₃ as compared to the single Nd³⁺ doped Y₂O₃. The emission peak at 563 nm is prominent in Er, Nd co-doped sample while no prominent visible emission is observed in Nd doped sample.

The upconversion emission mechanism is explained using the energy level diagram of both Nd³⁺ and Er³⁺ as shown in fig. 7. The absorption of 822 nm incident radiation excites Nd³⁺ ion via ground state absorption to ⁴F_{5/2}+²H_{9/2}. Further, emissions from Nd³⁺ ion occurs when it decays non-radiatively to metastable ⁴F_{3/2} from which it relaxed radiatively to the corresponding lower energy levels [21]. In the case of co-doped sample, Nd³⁺ ion transfer the part of absorbed energy to Er³⁺ via energy transfer (ET) process: ⁴F_{3/2}(Nd³⁺) + ⁴I_{15/2}(Er³⁺) → ⁴I_{9/2}(Nd³⁺) + ⁴I_{11/2}(Er³⁺) [22-23]. This leads to decrease in intensity in emission peaks corresponding to Nd³⁺ ion. Meanwhile, the lower energy level ⁴I_{13/2} of Er³⁺ is also populated because of nonradiative relaxation from upper ⁴I_{11/2} level [16]. The electrons in these two energy levels of Er³⁺ gets further excited to the higher excited states ⁴F_{3/2} and ²H_{11/2} via two excited state absorption (ESA) processes: ⁴I_{11/2}(Er³⁺) + E_{photon} → ⁴F_{3/2}(Er³⁺) and ⁴I_{13/2}(Er³⁺) + E_{photon} → ²H_{11/2}(Er³⁺), respectively. Finally, these populated Er³⁺ level relaxes dominantly through multi-phonon relaxation (MPR) by non-radiative transition to the

next lower levels ($^2H_{11/2}$, $^4S_{3/2}$ and $^4F_{9/2}$), which subsequently results in visible emission on radiative transitions from these states to the ground state.

Figure 8 shows Commission Internationale de l'Eclairage (CIE) diagram for $Y_2O_3:Er^{3+}(1at\%)Nd^{3+}(1at\%)$ sample. The calculated colour coordinates (x, y) are (0.355, 0.637). These values fall in yellowish-green region of CIE diagram.

Besides upconversion, the downconversion luminescence in both samples have been investigated. Figure 9 shows the excitation spectra measured in 300-400 nm range by monitoring emission at 1064 nm derived from $^4F_{3/2} \rightarrow ^4I_{11/2}$ transition of Nd^{3+} and the emission spectra using 357 nm as excitation wavelength derived from $^4I_{9/2} \rightarrow ^4D_{3/2}$ transition of Nd^{3+} . The near IR down-conversion material suitable for c-Si solar cell must be able to convert near UV (300-400 nm) part of solar spectrum to ~1000-1100 (band gap 1.12 eV) nm photons. The result shows, $Nd:Y_2O_3$ transparent ceramic is an efficient down-conversion material and hence had application for enhancing the efficiency of C-Si solar cell.

4. Conclusions

The Er^{3+} and Nd^{3+} co-doped Y_2O_3 transparent ceramics fabrication and infrared to visible frequency upconversion and near infrared downshifting has been investigated for the first time. The up-conversion was because of the energy transfer from Nd^{3+} to Er^{3+} ion, which are coexisted in Y_2O_3 host. Additional dopants Zr^{4+} and La^{3+} were used to increase sinter-ability of transparent ceramic. The phase formation, particle size and element composition were estimated using XRD, SEM and EDXRF measurement, respectively. The intrinsic characteristics of host Y_2O_3 involving its low photon energy, high thermal conductivity, broad transparency range, chemical and mechanical stability makes Er^{3+} and Nd^{3+} co-doped Y_2O_3 as promising dual mode efficient emitter. The obtained result in downconversion luminescence also put forward the possible use of the present transparent ceramic as spectral convertor in photovoltaics.

Acknowledgements

We thank Dr. Gurvinderjit Singh, Mr. S. K. Pathak (Laser Materials Section), Mr. M. P. Kamath and Mr. Pawan Kumar (Optical Design and Development Laboratory, Advanced Lasers & Optics Division) RRCAT, Indore for sintering and polishing of the pellets.

Table 1: Elemental Composition of the Particles using EDXRF

Sr No	Sample	Elements	Concentration (%)
1.	Y₂O₃: Nd,Zr,La	Nd	0.77 ± 0.1
		Y	96.84 ± 1
		La	1.00 ± 0.1
		Zr	1.39 ± 0.5
2.	Y₂O₃:Er,Nd,Zr,La	Er	1.25 ± 0.3
		Nd	0.72 ± 0.1
		Y	95.42 ± 1
		La	1.00 ± 0.1
		Zr	1.61 ± 0.5

Figure Captions:

Fig. 1. General strategy to achieve the upconversion and downshifting luminescence with Er/Nd codoped transparent ceramic.

Fig.2. X-ray diffraction pattern of $\text{Y}_2\text{O}_3:\text{Er}^{3+}(1\text{at}\%)$, $\text{Nd}^{3+}(1\text{at}\%)$ and $\text{Y}_2\text{O}_3:\text{Nd}^{3+}(1\text{at}\%)$ nanopowder.

Fig.3. FESEM image of (a) $\text{Y}_2\text{O}_3:\text{Er}^{3+}(1\text{at}\%)$, $\text{Nd}^{3+}(1\text{at}\%)$ and (b) $\text{Y}_2\text{O}_3:\text{Nd}^{3+}(1\text{at}\%)$ nanoparticles. (c) Particle size distribution of $\text{Y}_2\text{O}_3:\text{Er}^{3+}(1\text{at}\%)$, $\text{Nd}^{3+}(1\text{at}\%)$ and $\text{Y}_2\text{O}_3:\text{Nd}^{3+}(1\text{at}\%)$ nanoparticles.

Fig.4. Measured XRF spectra of $\text{Y}_2\text{O}_3:\text{Er}^{3+}(1\text{at}\%)$, $\text{Nd}^{3+}(1\text{at}\%)$ and $\text{Y}_2\text{O}_3:\text{Nd}^{3+}(1\text{at}\%)$ nanopowder.

Fig.5. The optical transmission spectra of $\text{Y}_2\text{O}_3:\text{Er}^{3+}(1\text{at}\%)$, $\text{Nd}^{3+}(1\text{at}\%)$ sintered pellet. Energy level transition corresponding to absorption in Nd^{3+} (in black) and Er^{3+} (in sky blue) are shown.

Fig.6. (a) The infrared excitation spectra of both [$\text{Y}_2\text{O}_3:\text{Er}^{3+}(1\text{at}\%)\text{Nd}^{3+}(1\text{at}\%)$] and $\text{Y}_2\text{O}_3:\text{Nd}^{3+}(1\text{at}\%)$] transparent ceramics by monitoring emission at 1064 nm. The peaks are assigned corresponding to their energy transitions. (b) The PL emission spectra, under 822 nm excitation, of $\text{Y}_2\text{O}_3:\text{Er}^{3+}(1\text{at}\%)\text{Nd}^{3+}(1\text{at}\%)$ and $\text{Y}_2\text{O}_3:\text{Nd}^{3+}(1\text{at}\%)$ samples in 420-1700 nm range. The peaks are assigned corresponding to their energy level transitions.

Fig.7. Possible energy level diagram of Nd^{3+} and Er^{3+} .

Fig. 8. Color coordinates of upconversion emission of $\text{Y}_2\text{O}_3:\text{Er}^{3+}(1\text{at}\%)\text{Nd}^{3+}(1\text{at}\%)$ transparent ceramics under 822 nm excitation in 1931 CIE diagram.

Fig.9. Near UV excitation spectra of both [$\text{Y}_2\text{O}_3:\text{Er}^{3+}(1\text{at}\%)\text{Nd}^{3+}(1\text{at}\%)$] and $\text{Y}_2\text{O}_3:\text{Nd}^{3+}(1\text{at}\%)$] transparent ceramics measured by monitoring emission at 1064 nm. The PL emission spectra, observed under 357 nm excitation of both samples in 400 -1500 nm range. The peaks are assigned corresponding to involved energy transitions in Nd^{3+} and Er^{3+} ions.

References:

- [1] Adolf Giesen and Jochen Speiser, Fifteen Years of Work on Thin-Disk Lasers: Results and Scaling Laws, *IEEE J. Sel. Topics Quantum Electron.*, 13 (2007) 3.
- [2] Akio Ikesue and Yan Lin Aung, Ceramic laser materials, *Nat. Photon.*, 2 (2008) 721.
- [3] Lin Gan, Young-Jo Parka, Lin-Lin Zhu, Shin-II Go, Haneul Kim, Jin-Myung Kim, Jae-Woong Ko, Fabrication and properties of La₂O₃-doped transparent yttria ceramics by hot-pressing sintering, *J Alloys Compd.*, 695 (2017) 2142.
- [4] Andrzej Kruk, Optical and structural properties of arc melted Ce or Pr –doped Y₂O₃ transparent ceramics, *Ceram. Int.*, 43 (2017) 16909.
- [5] Zhengfa Dai, Qiang Liu, Guido Toci, Matteo Vannini, Angela Pirri, Vladimir Babin, Martin Nikl , Wei Wang, Haohong Chen, Jiang Li, Fabrication and laser oscillation of Yb:Sc₂O₃ transparent ceramics from coprecipitated nano-powders, *J. Eur. Ceram. Soc.*, Accepted 15 October 2017, doi: 10.1016/j.jeurceramsoc.2017.10.027
- [6] V. Lupei, A. Lupei, S. Hau, C. Gheorghe, A. Ikesue, Structural and electron-phonon interaction effects in optical spectra of Pr³⁺ and Sm³⁺ in YAG, *J Alloys Compd.*, 706 (2017) 176.
- [7] Ling Bing Kong, Y. Z. Huang, W. X. Que, T. S. Zhang, S. Li, J. Zhang, Z. L. Dong, D. Y. Tang, *Transparent Ceramics*, Springer, 2015, ISBN: 978-3-319-18955-0.
- [8] H. Schafer and M. Haase, “Upconverting Nanoparticles”, *Angew. chem. Int. Ed.* 50 (2011) 5808.
- [9] R. Scheps, Upconversion laser processes, *Prog. Quantum Electron.*, 20 (1996)271.
- [10] W. R. Zipfel, R. M. Williams, R. Christie, A. Yu Nikitin, B. T. Hyman, W. W. Webb, Live tissue intrinsic emission microscopy using multiphoton-excited native fluorescence and second harmonic generation, *Proc. Natl. Acad. Sci. USA*, 100 (2003) 7075.
- [11] Jing Zhou, Qian Liu, Wei Feng, Yun Sun, and Fuyou Li, Upconversion Luminescent Materials: Advances and Applications, *Chem. Rev.* 115 (2015) 395.
- [12] Y F Wang, G Y Liu, L D. Sun, J W Xiao, J C Zhou, C H Yan, Nd³⁺-sensitized upconversion nanophosphors: efficient In vivo bioimaging probes with minimized heating effect, *ACS Nano*, 7 (2013)7200.
- [13] Xiaomin Li, Rui Wang, Fan Zhang, Lei Zhou, Dengke Shen, Chi Yao & Dongyuan Zhao, Nd³⁺ sensitized up/down converting dual-mode nanomaterials for efficient in-vitro and in-vivo bioimaging excited at 800 nm, *Sci. Rep.*,3 (2013) 3536.

- [14] P. Deshmukh, S. Satapathy, M.K. Singh, Y.P. Kumar, P.K. Gupta, Tb³⁺/Yb³⁺ co-doped Y₂O₃ upconversion transparent ceramics: Fabrication and characterization for IR excited green emission, *J. Eur. Ceram. Soc.*, 37(2017) 239.
- [15] Pratik Deshmukh, S. Satapathy, Anju Ahlawat, M. K. Singh, P. K. Gupta, A. K. Karnal, (Yb_{0.01}Zr_{0.02}La_{0.01}Y_{0.96})₂O₃ transparent ceramic: fabrication, structural and optical characterization for IR emission”, *J Mater Sci: Mater Electron*, DOI: 10.1007/s10854-017-6885-7.
- [16] M. K. Tiwari , P. Gupta , A. K. Sinha, S. R. Kane, A. K. Singh , S. R Garg, C. K. Garg, Lodha, G S, Deb S K: A microfocus X-ray fluorescence beamline at Indus-2 synchrotron radiation facility, *J. Synchrotron Radiat.* 20 (2013) 386.
- [17] M K Tiwari, A K Singh and K J S Sawhney, Analysis of Stainless Steel Samples By Energy Dispersive X-Ray Fluorescence (EDXRF) Spectrometry, *Indian Academy Of Sciences.633, Bull. Mater. Sci.* 24 (2001) 633.
- [18] J. Yuan, S. X. Shen, D. D. Chen, Q. Qian, M. Y. Peng, and Q. Y. Zhang, Efficient 2.0 μm emission in Nd³⁺/Ho³⁺ co-doped tungsten tellurite glasses for a diode-pump 2.0 μm laser, *J. Appl. Phys.*113 (2013) 173507.
- [19] Shenzhou Lu, QiuHong Yang , Bin Zhang, Haojia Zhang , “Upconversion and infrared luminescences in Er³⁺/Yb³⁺ codoped Y₂O₃ and (Y_{0.9}La_{0.1})₂O₃ transparent ceramics”, *Opt. Mater.* 33 (2011) 746.
- [20] Fangze Chen, Tao Wei, Xufeng Jing, Ying Tian, Junjie Zhan, Shiqing Xu, Investigation of mid-infrared emission characteristics and energy transfer dynamics in Er³⁺ doped oxyfluoride tellurite glass, *Sci. Rep.*5 (2015)10676.
- [21] Prasenjit Prasad Sukul and Kaushal Kumar, Near-infrared (808 and 980 nm) excited photoluminescence study in Nd-doped Y₂O₃ phosphor for bio-imaging, *Methods Appl. Fluoresc.*, 4(2016) 044005.
- [22] Bao-Cheng Wang, Cheng-Ren Li, Bin Dong , Li Zhang Wei Xu, Application to temperature sensor based on near infrared emissions of Nd³⁺:Er³⁺:Yb³⁺ co-doped Al₂O₃, *Optical Engineering* 48 (2009)104401.
- [23] Yanfeng Zheng, Baojiu Chen, Haiyang Zhong, Jiashi Sun, Lihong Cheng, Xiangping Li, Z Jinsu Zhang, Yue Tian, Weili Lu, Jing Wan, Tingting Yu, Libo Huang, Hongquan Yu, and Hai Liny, “Optical Transition, Excitation State Absorption, and Energy Transfer Study of Er³⁺,

Nd³⁺ Single-Doped, and Er³⁺/Nd³⁺ Codoped Tellurite Glasses for Mid-Infrared Laser Applications”, *J. Am. Ceram. Soc.*, 94 (2011)1766.

Figure 1:

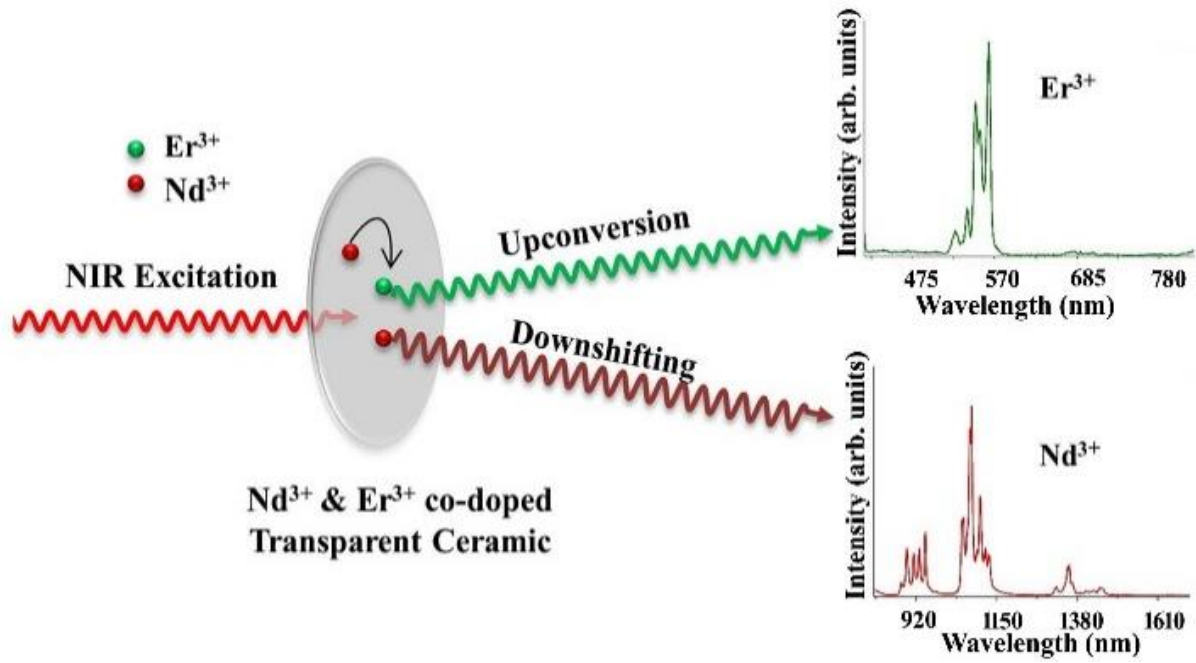


Figure 2:

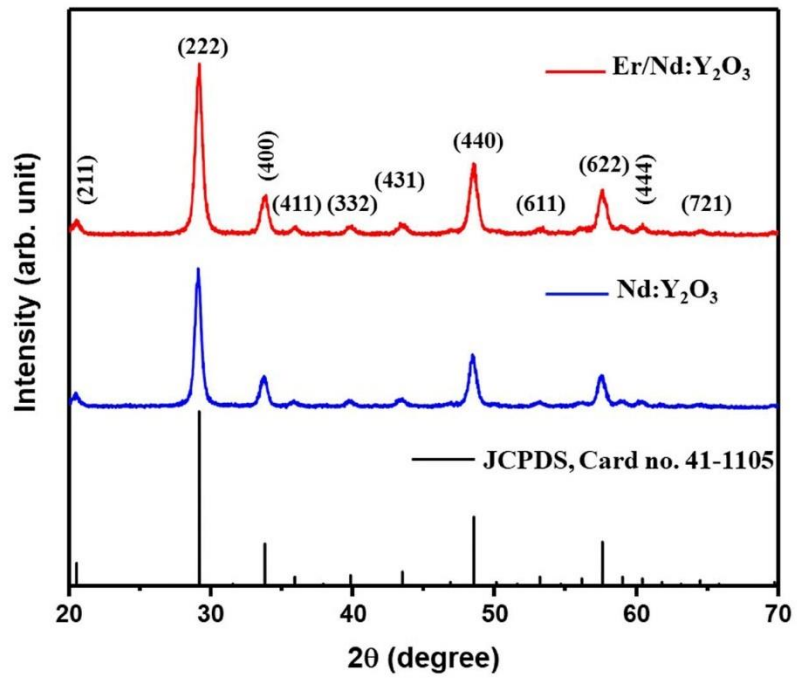


Figure 3:

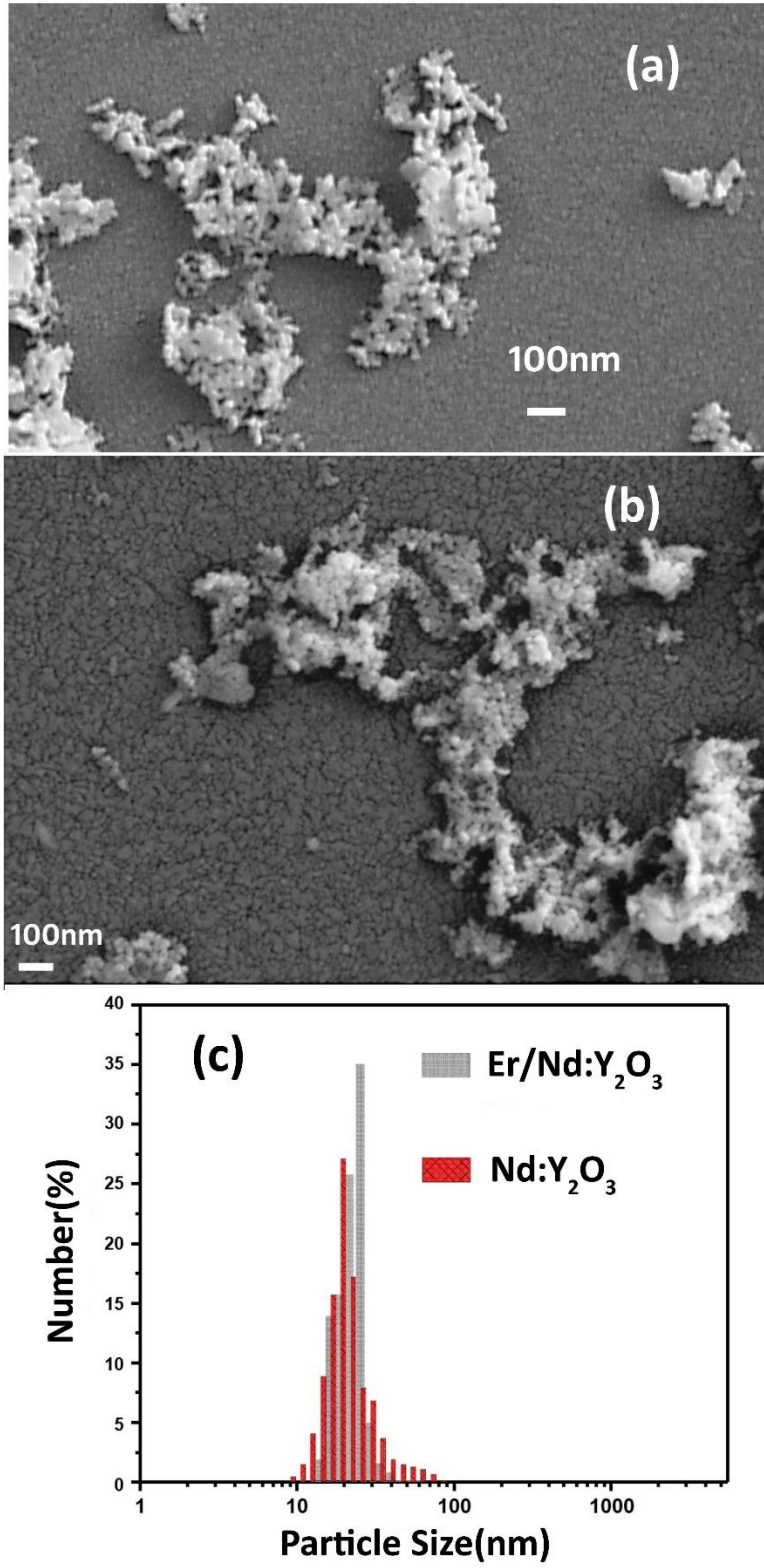


Figure 4:

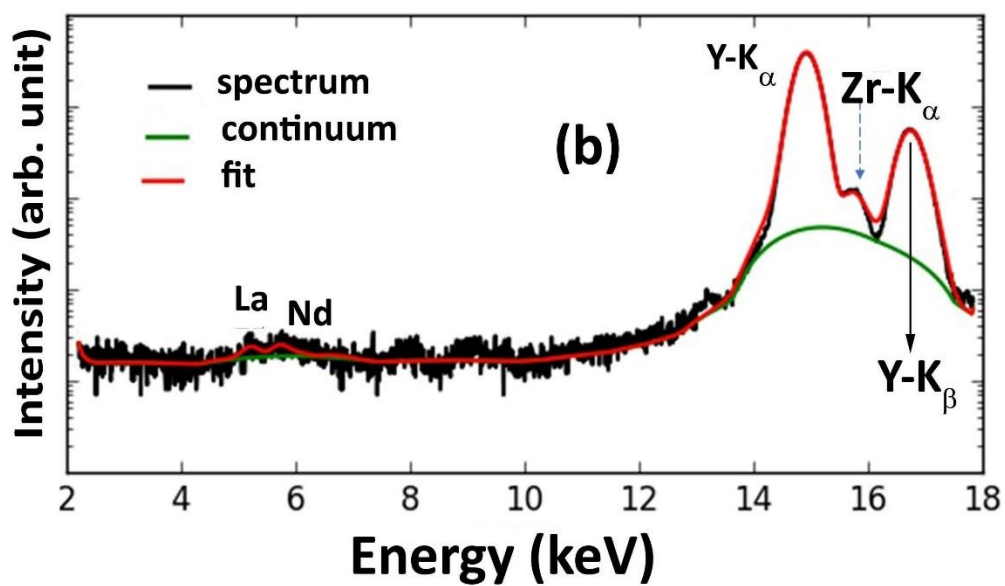
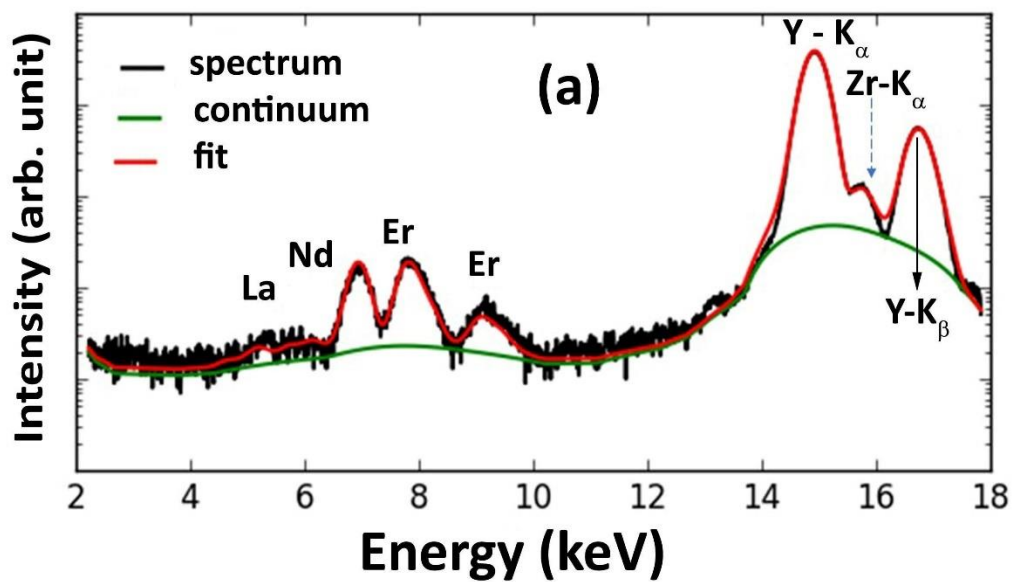


Figure 5:

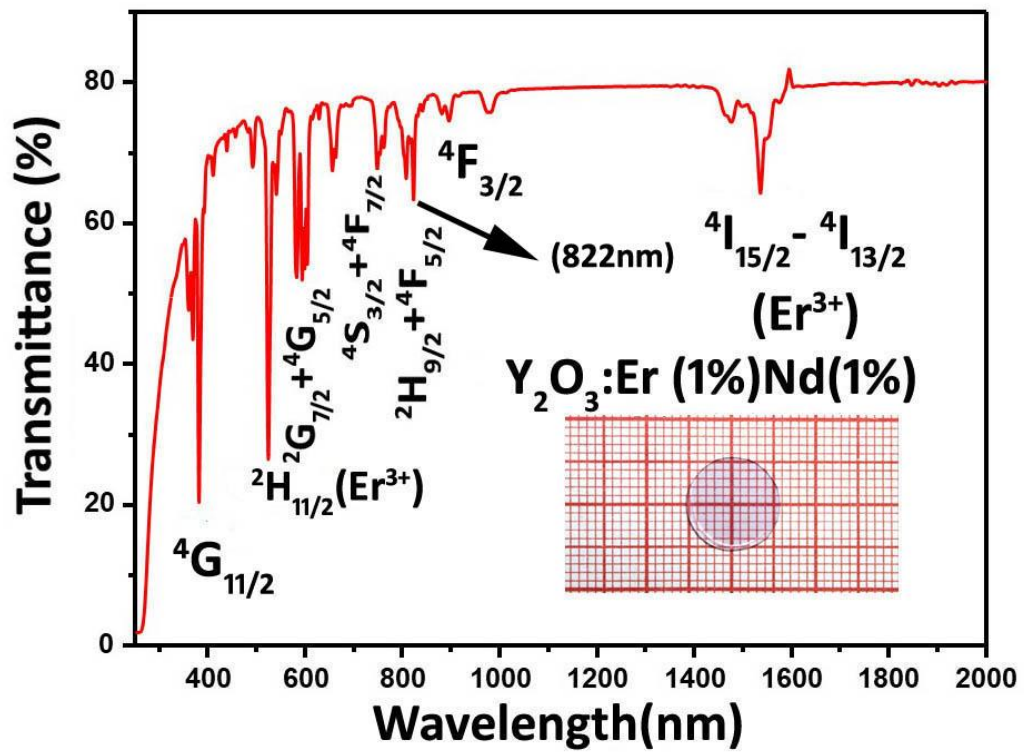


Figure 6:

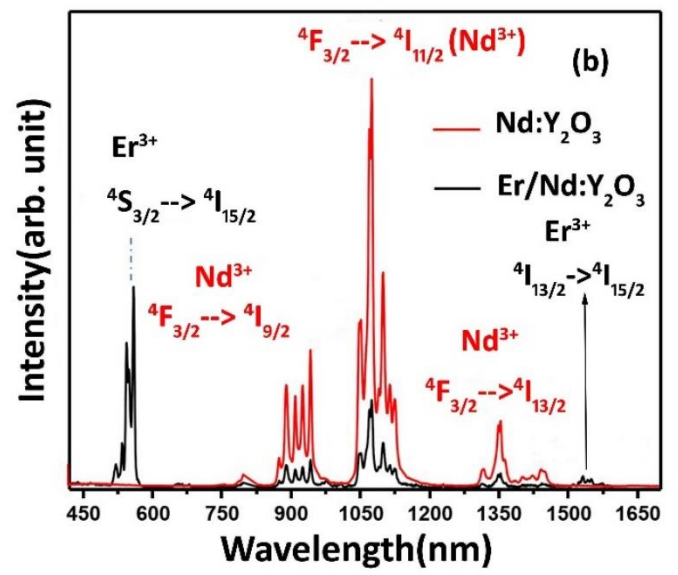
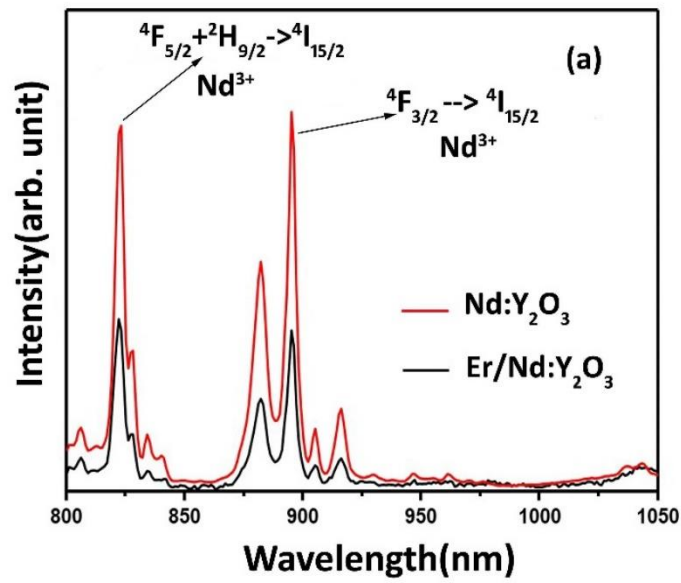


Figure 7:

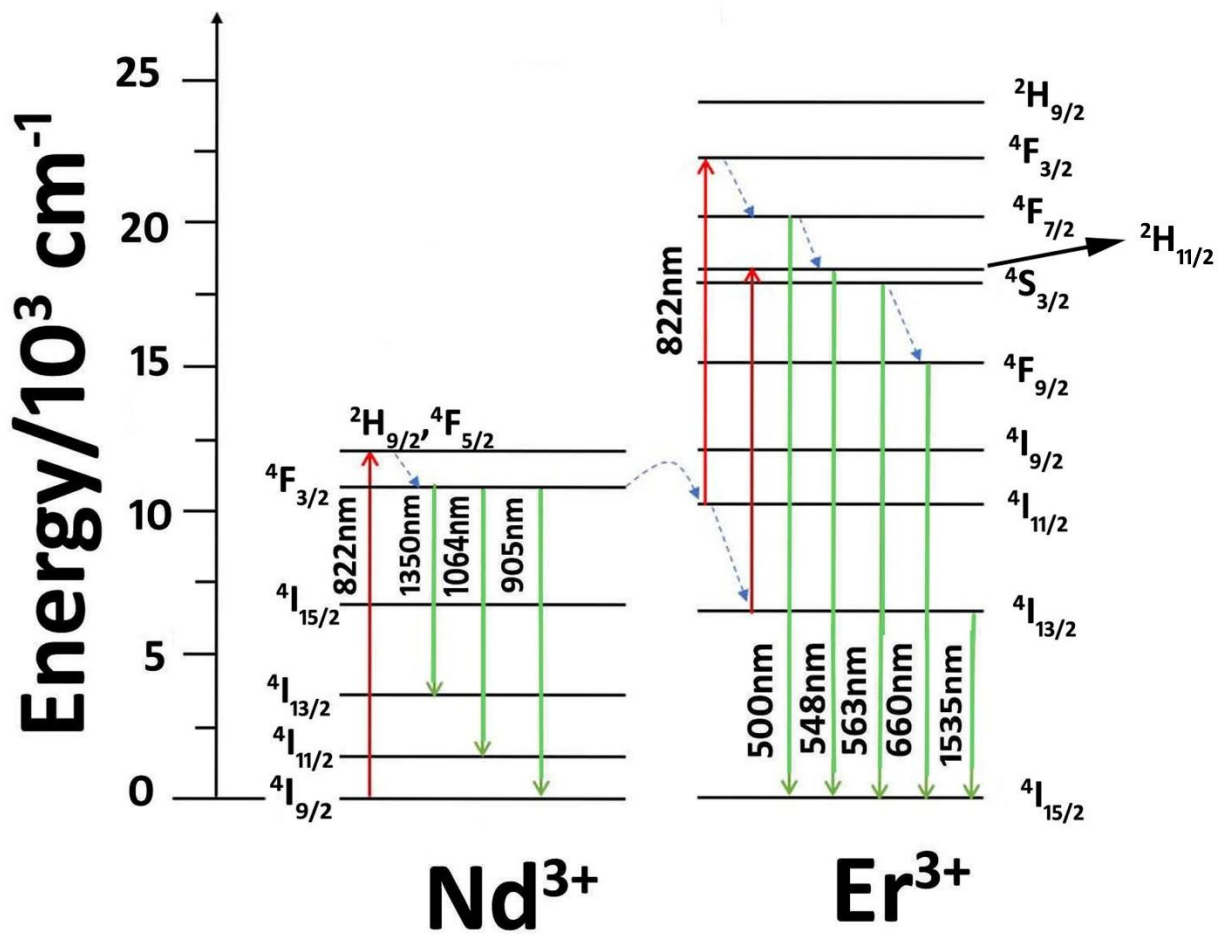


Figure 8:

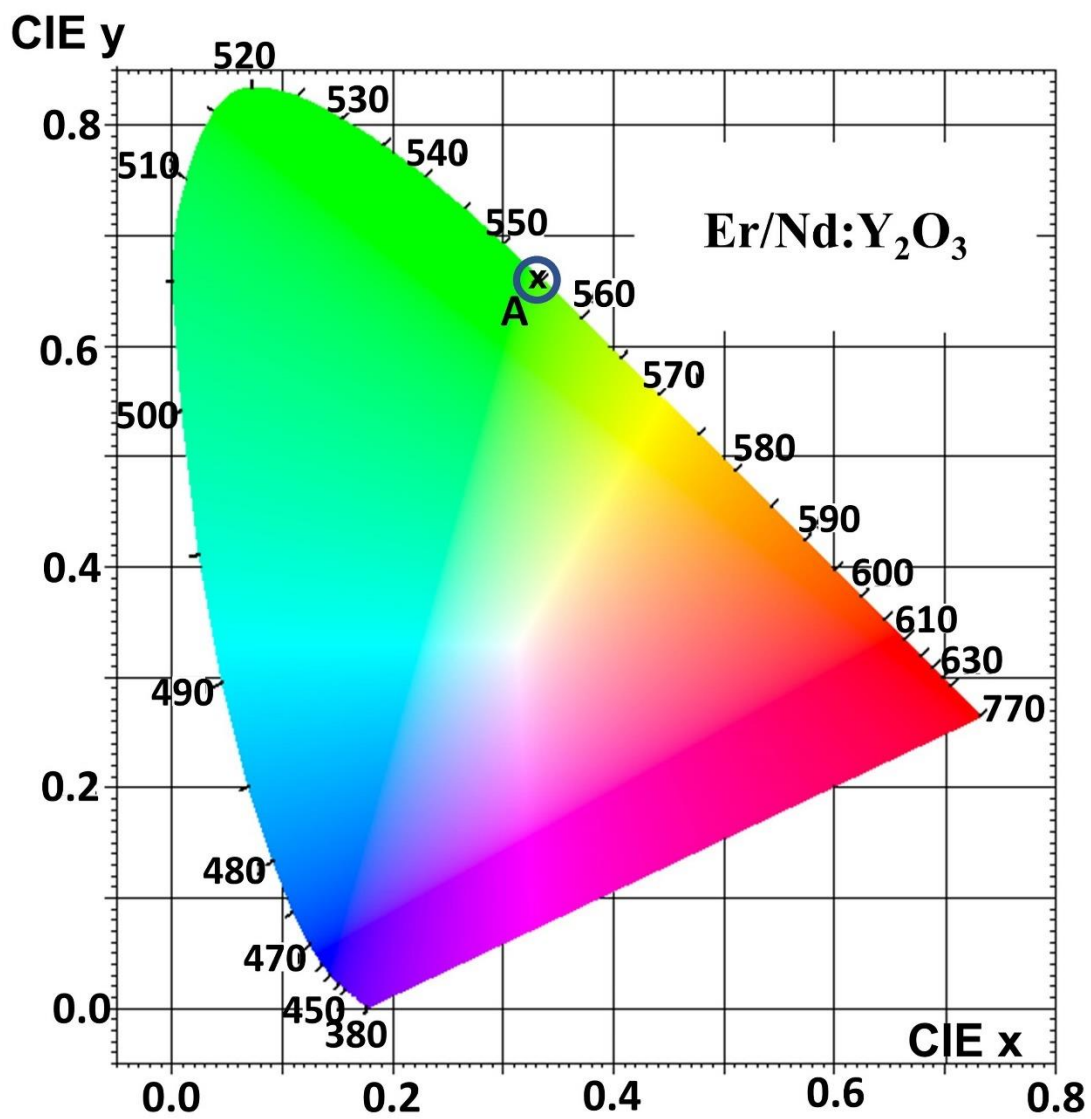


Figure 9:

Intensity (arb. unit)

